Restoring Lost Cognitive Function

Hippocampal-Cortical Neural Prostheses

BY THEODORE W. BERGER, ASHISH AHUJA, SPIROS H. COURELLIS, SAMUEL A. DEADWYLER, GOPAL ERINJIPPURATH, GREGORY A. GERHARDT, GHASSAN GHOLMIEH, JOHN J. GRANACKI, ROBERT HAMPSON, MIN CHI HSAIO, JEFFREY LACOSS, VASILIS Z. MARMARELIS, PATRICK NASIATKA, VIJAY SRINIVASAN, DONG SONG, ARMAND R. TANGUAY, AND JACK WILLS

One of the frontiers in the biomedical sciences is the development of prostheses for the central nervous system (CNS) to replace higher thought processes that have been lost due to damage or disease. Prosthetic systems that interact with the CNS are currently being developed by several groups [1], though virtually all other CNS prostheses focus on sensory or motor system dysfunction and not on restoring cognitive loss resulting from damage to central brain regions.

Systems designed to compensate for the loss of sensory input attempt to replace the transduction of physical energy from the environment into electrical stimulation of sensory nerve fibers (e.g., a cochlear implant or artificial retina) or the sensory cortex [2]–[4]. Systems designed to compensate for the loss of motor control do so through functional electrical stimulation (FES), in which preprogrammed stimulation protocols are used to activate muscular movement [5], [6], or by decoding premotor/motor cortical commands for the control of robotic systems [7]–[9].

The type of neural prosthesis that performs or assists a cognitive function is qualitatively different from the cochlear implant, artificial retina, or FES. We consider here a prosthetic device that functions in a biomimetic manner to replace information transmission between cortical brain regions [10], [11]. In such a prosthesis, damaged CNS neurons would be replaced with a biomimetic system comprised of silicon neurons. The replacement silicon neurons would have functional properties specific to those of the damaged neurons and would both receive as inputs and send as outputs electrical activity to regions of the brain with which the damaged region previously communicated (Figure 1). Thus, the class of prosthesis being proposed is one that would replace the computational function of the damaged brain and restore the transmission of that computational result to other regions of the nervous system. Such a new generation of neural prostheses would have a profound impact on the quality of life throughout society; it would offer a biomedical remedy for the cognitive and memory loss accompanying Alzheimer's disease, the speech and language deficits resulting from stroke, and the impaired ability to execute skilled movements following trauma to brain regions responsible for motor control.

The Hippocampal System: Basis for Long-Term Declarative Memory

We are in the process of developing such a cognitive prosthesis for the hippocampus, a region of the brain involved in the formation of new long-term memories. The hippocampus is responsible for what have been termed long-term *declarative* or *recognition* memories [12]–[18]: the formation of mnemonic labels that identify a unifying collection of features (e.g., those comprising a person's face) and form relations between multiple collections of features (e.g., associating the visual features of a face with the auditory features of the name for that face). It is the degeneration and malformation of hippocampal neurons that is the underlying cause of the memory disorders associated with Alzheimer's disease. Similarly, hippocampal pyramidal cells, particularly those in region CA1, are highly susceptible to even brief periods of anoxia, such as those that accompany stroke. Even blunt head trauma has been shown to be associated with a preferential loss of hippocampal neurons in the hilus of the dentate gyrus. Finally, there is a long history of association between hippocampal dysfunction (particularly in region CA3) and epileptiform activity. Thus, there is a wide array of neural damage and neurodegenerative disease conditions for which a hippocampal prosthesis would be clinically relevant.

The hippocampus comprises several different subsystems that form a closed feedback loop (Figure 2); input from the neocortex enters via the entorhinal cortex, propagates through the intrinsic subregions of hippocampus, and then returns to the neocortex. The intrinsic pathways consist of a cascade of excitatory connections organized roughly transverse to the longitudinal axis of the hippocampus. As such, the hippocampus can be conceived of as a set of interconnected, parallel circuits [19], [20]. The significance of this organizational feature is that, after removing the hippocampus from the brain, transverse slices (400 μm thick) of the structure may be maintained in vitro that preserve a substantial portion of the intrinsic circuitry.

Proof-of-Concept: Replacement of the CA3 Region of the Hippocampal Slice with a Biomimetic Device

We have developed a multistage plan for achieving a neural prosthesis for the hippocampus. The first stage involves a

 0739-5175/05/$20.00©2005IEEE

proof of concept in which we develop a replacement biomimetic model of the CA3 subregion of hippocampal in vitro slice. We have chosen to realize our first-generation prosthesis in the context of a hippocampal slice for several reasons. Among these is that the 400-μm thickness of the slice allows us, essentially, to reduce the problems of modeling the three-dimensional (3-D) function of the hippocampus and of interfacing with its complex, 3-D structure to a more tractable two-dimensions. This allows us to develop the initial stages of experimental strategies, modeling methodologies, hardware designs, and interfacing technologies within the context of a more simplified and controlled set of conditions.

The major intrinsic circuitry of the hippocampus consists of an excitatory cascade of the dentate, CA3, and CA1 subregions [Figure 3(a)] and is maintained in a slice preparation. Our Stage 1 prosthesis demonstration consists of: 1) surgically eliminating the CA3 subregion, 2) replacing the biological CA3 with a very large-scale integrated (VLSI)-based model of the nonlinear dynamics of CA3 [Figure 3(b) and (c)], and 3) through a specially designed multisite electrode array, transmitting dentate output to the VLSI model and VLSI model output to the inputs of CA1 [Figure 3(c)]. The definition of a successful implementation of the prosthesis is the propagation of spatio-temporal patterns of activity from dentate→VLSI model→CA1 reproduces that observed experimentally in the biological dentate→CA3→CA1 circuit. The remainder of this article will detail the current progress in implementing the Stage 1 prosthesis for the hippocampal slice.

Experimental Characterization and Mathematical Modeling of the Nonlinear Dynamic Properties of the Hippocampal CA3 Region

Our strategy for achieving a hippocampal neural prosthesis is based on several system requirements for replacing any CNS region with a biomimetic device that interacts bidirectionally with the rest of the undamaged brain (i.e., sensing and communicating input to the biomimetic device from afferents of the damaged region and communicating and electrically stimulating outputs from the biomimetic device to efferents of the damaged region) [10], [11].

The most important component is the nature of the biomimetic model that constitutes the core of the prosthetic system. Information in the hippocampus and all other parts of the brain is coded in terms of variation in the sequence of all-or-none, point-process (spike) events, or temporal pattern (for multiple neurons,

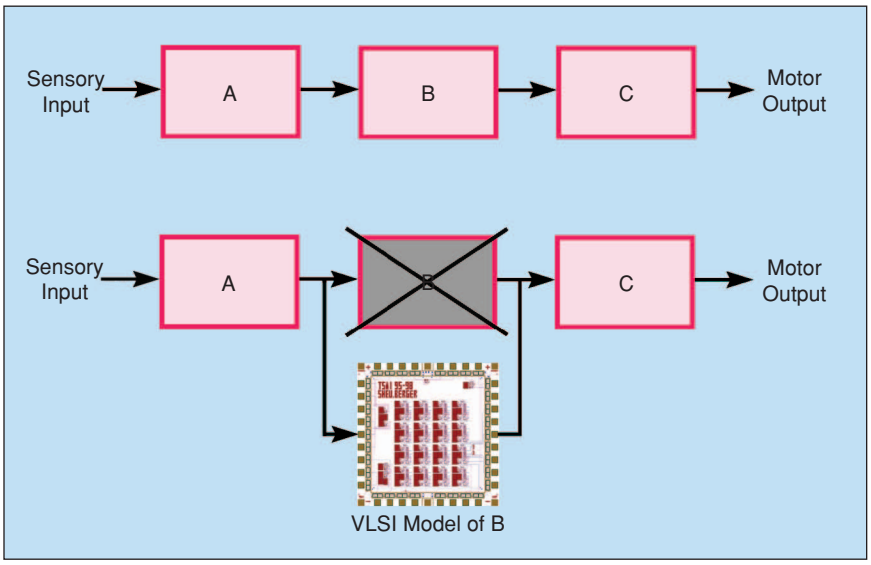

Fig. 1. A schematic diagram for the general case of replacing a damaged central brain region with a VLSI system implementation of a biomimetic model, and connecting the inputs of the VLSI-based model to the afferents of the damaged region and the outputs of the VLSI-based model to the efferents of the damaged region.

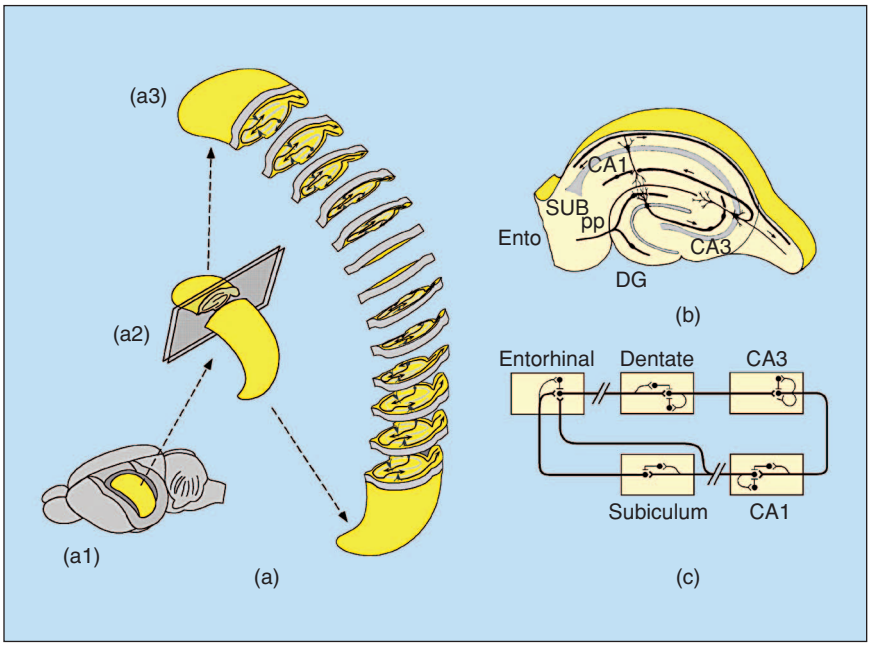

Fig. 2. (a) Diagrammatic representation of the rat brain (a1), showing the relative location of the hippocampal formation on the left side of the brain; diagrammatic representation of the left hippocampus after isolation from the brain (a2), and slices of the hippocampus for sections transverse to the longitudinal axis (a3). (b) and (c) Diagrammatic representation of one transverse slice of hippocampus, illustrating its intrinsic organization: fibers from the entorhinal cortex (ENTO) project through perforant path (pp) to the dentate gyrus (DG); granule cells of the dentate gyrus project to the CA3 region, which in turn projects to the CA1 region; CA1 cells project to the subiculum (SUB), which in the intact brain then projects back to the entorhinal cortex.

variation in the spatio-temporal pattern). The essential signal processing capability of a neuron is derived from its capacity to change an input sequence of interspike intervals into a different output sequence of interspike intervals (or amplitude-time course synaptic potentials). In all brain areas, the resulting input/output transformations are strongly nonlinear because of the nonlinear dynamics inherent in the cellular/molecular mechanisms comprising neurons and their synaptic connections [21]–[23]. As a consequence, the output of virtually all neurons in the brain is highly dependent on temporal properties of the input. Thus, identifying the nonlinear input/output (I/O) properties of hippocampal neurons and the composite I/O transformations of hippocampal circuitry is the fundamental functionality that must be captured by any mathematical model designed to replace damaged hippocampal tissue.

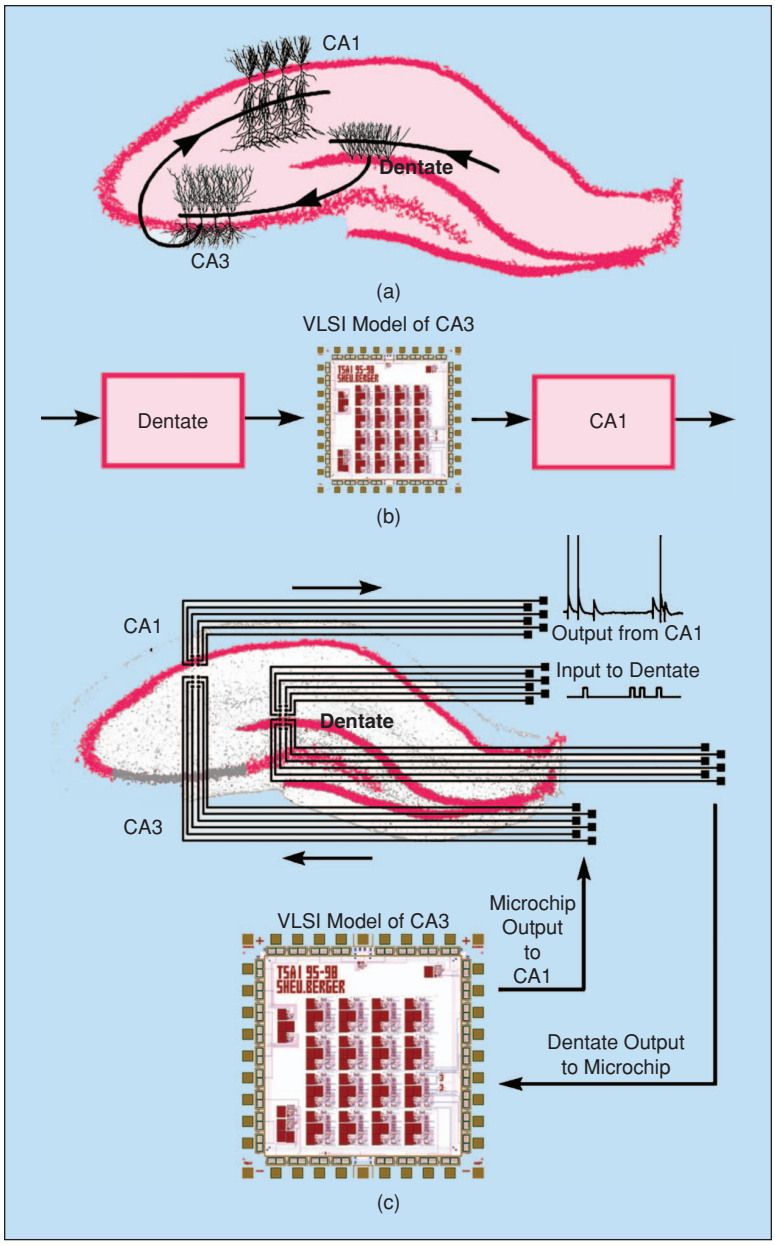

Fig. 3. A strategy for replacing the CA3 region of hippocampus with a VLSI model of its nonlinear dynamics and interfacing the VLSI biomimetic device with the remaining, active slice through a conformal, multisite electrode array, thus restoring whole-circuit dynamics; (a) diagrammatic representation of the trisynaptic circuit of the hippocampus; (b) conceptual representation of replacing the CA3 field with a VLSI-based model; (c) hippocampal slice in which the CA3 field has been removed. Overlaid is an integrated system in which impulse stimulation from an external source is used activate dentate granule cells and is delivered through one component of a multisite electrode array. A second component of the electrode array senses the responses of dentate granule cells and transmits the responses to the VLSI-based model. The VLSI device performs the same nonlinear I/O transformations as biological CA3 neurons and transmits the output through the multisite electrode array to the dendrites of CA1 neurons, thus activating the last component of the trisynaptic pathway.

Attempting to accomplish this modeling goal with compartmental neuron models [24], [25] based on cable theory is simply not feasible. The number of parameters required to represent complex dendritic structures and the number and variety of ligand- and voltage-dependent conductances common to hippocampal neurons is simply too large to include in a multineuron network model that is sufficiently compact for a microchip or even a multichip module. Although simplifications of compartmental neuron models are an option, the trade-offs between the complexity of the model and representation of neuron and network dynamics are not yet fully understood [26]. For this reason, we are using a nonlinear systems analytic approach to modeling hippocampal neurons [21]–[23], [27]–[32]. In this approach, neurons and circuits or networks to be modeled are first characterized experimentally using a broad-band stimulus, e.g., a series of impulses (typically 1,000–2,000 total) in which the interimpulse intervals vary according to a random (Poisson) process. Because the distribution of interimpulse intervals is exponential, the mean frequency can remain relatively low (2 Hz), and thus be physiological, yet the range of intervals can be wide (10–5,000 ms). Such a stimulation protocol ensures that the majority, if not all, of synaptic and cellular mechanisms are activated, and as a consequence, contribute to neuron, circuit, or network output which is measured (e.g., electrophysiologically). The modeling effort, identified as the Volterra-Poisson modeling approach, then becomes focused on estimating linear and nonlinear components of the mapping of the known input to the experimentally measured output. The Volterra modeling approach is a mathematically rigorous, scalable method [33], [34] that can be applied to biological systems [35]. The nonlinear dynamic I/O characteristics of the modeled system are quantitatively captured by the Volterra kernels. Volterra kernels are system descriptors that remain invariant with respect to the type or the power of the stimulus. Given accurate estimation methods [27], [36], [37], the result is a compact (many

fewer terms than a compartmental neuron network model) and predictive (for virtually any temporal pattern) model that incorporates at least the majority of known and unknown biological mechanisms (thus, not requiring modification and optimization for each new discovery in the future).

Accordingly, our first step in developing a prosthesis for the hippocampus is to experimentally characterize the nonlinear I/O properties both of field CA3 and of the entire trisynaptic pathway, i.e., the combined nonlinearities due to propagation through the dentate→CA3→CA1 subfields. The model of CA3 will be used to develop the biomimetic replacement device to substitute for CA3 dynamics after the biological CA3 has been removed from the slice. The I/O properties of the trisynaptic pathway will be used to evaluate the extent to which hippocampal circuit dynamics have been restored after substituting the biomimetic device for field CA3. Random impulse train stimulation is applied only to the perforant path afferents to dentate. Nonlinearities of the dentate then determine the actual input to CA3; in turn, the nonlinearities of CA3 determine the input to CA1. Field potentials are used as the measure of output from each of the three hippocampal regions: population spikes of dentate granule cells, population spikes of CA3 pyramidal cells, and population EPSPs (excitatory postsynaptic potentials) of CA1 pyramidal cells. Thus, for both fields CA3 and CA1, not only does the continuous input of the random train vary in terms of interimpulse interval, but because of nonlinearities upstream, the input also varies in terms of the number of active afferents. This places a major constraint on modeling CA3 input/output properties, i.e., the model must be capable of predicting CA3 output as a function of both the temporal pattern and the amplitude of dentate input.

A small segment of one random train and the evoked dentate, CA3, and CA1 field potential responses are shown in Figure 4. The first trace [Figure 4(b)] represents the impulse stimulations used to activate perforant path (pp in the upper panel) afferents to dentate (DG). The strong nonlinearities of the dentate are evident in the second trace [Figure 4(c)]; the amplitude of the negative-going population spike varies considerably as a function of interimpulse interval. Likewise, CA3 population spikes and CA1 population EPSPs also exhibit strong variation in amplitude as a function of the temporal intervals of the train. It is the dependence of CA3 output on interimpulse interval and dentate population amplitude that must be captured by the model.

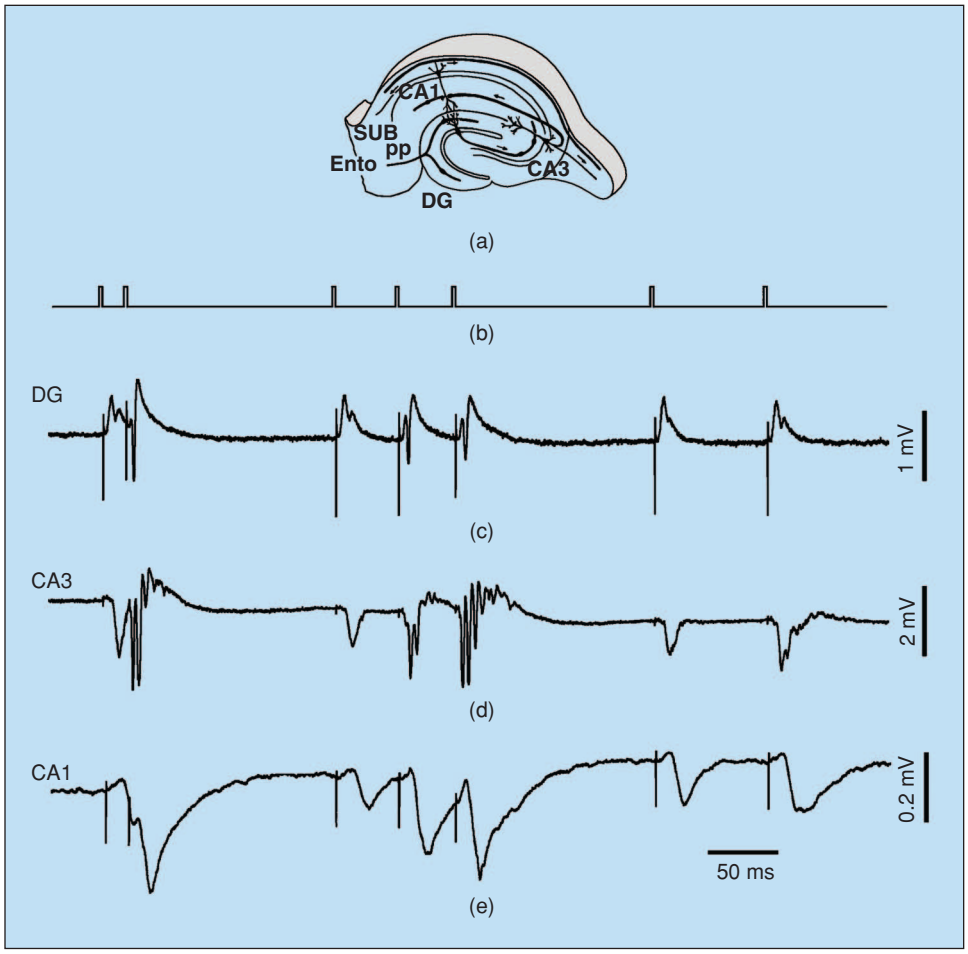

Fig. 4. (a) Diagrammatic representation of a hippocampal slice (from Andersen). (b) Segment of a series of impulses with randomly varying interimpulse intervals delivered in one in vitro hippocampal slice experiment to perforant path (pp) fibers originating from the entorhinal cortex (ENTO) and terminating in the dentate gyrus (DG). (c) Field potential responses recorded from the DG. The narrow, biphasic deflections preceding the field potential responses are stimulation artifacts and, therefore, correspond to the occurrence of stimulation impulses in the first trace. The large negative-going deflection in each response is the "population spike." The amplitude of the population spike correlates positively with the number of granule cells reaching threshold and generating an action potential. It is the amplitude of the population spike that is used as the measure of output from both DG and CA3. (d) Field potential responses recorded from CA3. The stimulation artifacts are much smaller in amplitude. Note the occurrence of multiple population spikes, which is presumed to be due to excitatory, recurrent collaterals unique to the CA3 field. (e) Field potential responses recorded from CA1. These responses are recorded from the dendritic region of CA1 and thus reflect population excitatory synaptic potential responses (EPSPs) of CA1 neurons rather than population action potentials ("population spikes"). Note the progressively longer delay in the onset of response following the stimulation artifact for fields DG, CA3, and CA1, reflecting the propagation of activity through the hippocampal trisynaptic circuit.

These experimental datasets of population spike sequences recorded at the granule cell layer (input) and the corresponding population spike sequences recorded at the pyramidal cell layer of CA3 (output) were used to estimate the Volterra-Poisson model of CA3. The model estimation was carried out using only the amplitude and the interspike intervals of the population spikes in the input and output sequences [Figure 5(a)]. The equation representing the single input/single output, third-order Volterra-Poisson model employed to capture the CA3 nonlinear dynamic properties was adapted as follows:

$$y(n_i) = A_i k_1 + A_i \sum_{n_i-\mu<n_j<n_i} A_j k_2(n_i - n_j) + A_i \sum_{n_i-\mu<n_{j_1}<n_i} \sum_{n_i-\mu<n_{j_2}<n_i} A_{j_1} A_{j_2} k_3(n_i - n_{j_1}, n_i - n_{j_2})$$

where A_i, A_j represent the varying amplitudes of the population spikes recorded at the granule cell layer (input), $y(n_i)$ represents the amplitude of the population spikes recorded at CA3 (output), k_1, k_2, and k_3 are the first, second, and third-order kernels respectively, n_i is the time of occurrence of the current impulse in the I/O sequence, and n_j is the time of occurrence of the jth impulse prior to the present impulse within the kernel's memory window μ.

The estimation of the kernels is facilitated by expanding them on the orthonormal basis of Laguerre polynomials, the coefficients of which can be obtained via least-squares method as described previously [36]. Data collected from hippocampal slices were analyzed and the associated Volterra-Poisson kernels were computed. A third-order model was selected as it provided a consistent improvement in normalized mean square error (NMSE) between 4–9%, compared to a second-order model. The class of computed kernels with consistently low NMSE in the neighborhood of 6% exhibited behavior similar to the representative case shown in Figure 5(b). In particular, the second-order kernels exhibited a fast depressive phase in the beginning followed by a brief facilitatory phase and a slow, shallow depressive phase before returning to the zero line. The third-order kernels exhibited a fast facilitatory phase in the beginning followed by slower and shallower depressive and facilitatory phases before returning to the zero plane.

One of the most important properties of a Volterra-Poisson model is its predictive capability to arbitrary input patterns. It is a property that is necessary for the CA3 model to function as a CA3 replacement, since it is not bound to a specific input sequence. Each value predicted by the Volterra-Poisson model is the result of the nonlinear functional terms of the corresponding Volterra-Poisson series. The nth-term of the series contributes to the computation of the predicted output with the effect of nth-order interactions among the input impulses weighed by the nth-order kernel across its memory window.

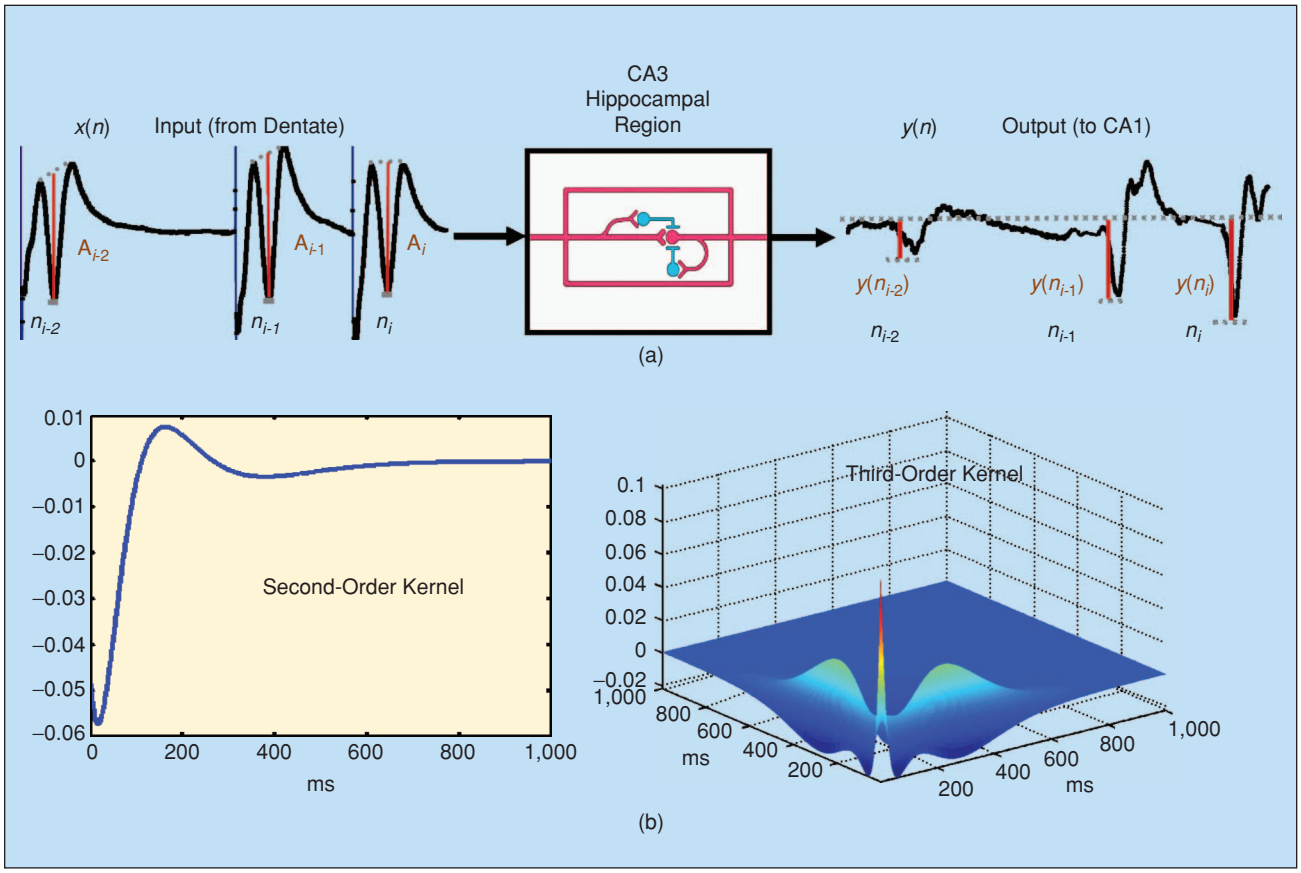

Fig. 5. (a) The nonlinear dynamic model of the CA3 hippocampal region receives input $x(n)$ from the dentate, a Poisson point process with events (electrical impulses) of variable amplitude (A_i), and randomly varying interimpulse intervals and generates a series $y(n)$ of variable amplitude point-process events synchronous to the input. (b) A representative second-order kernel (left) and third-order kernel (right) of the CA3 nonlinear dynamic mapping.

An example of how each term of the Volterra-Poisson model of the CA3 contributes to the computation of predicted output of the model is shown in Figure 6. The small NMSE values (on the order of 6%) observed during the analysis for the selected class of models indicate that the kernels computed from the experimental data sets reliably captured the CA3 nonlinear dynamics and that the prediction accuracy of the resulting CA3 model is high. An example of model prediction using the Volterra-Poisson model developed for CA3 using the slice experimental data is shown in Figure 7.

Hardware Implementation of the Nonlinear Model of Hippocampal CA3

A biomimetic model of a hippocampal network of neurons must be reduced to a hardware implementation in a microcircuitry VLSI system for at least three reasons. First, for a neural prosthetic device used clinically, it will be necessary to simulate multiple neurons and neural circuits in parallel; hardware implementations provide the most efficient means for realizing parallel processing. Second, by definition, the device in question will be required to interact with the intact brain in real time if it is to substitute for lost neural function and at least partially reinstate normal levels of cognition and behavior. Again, the rapid operational rates of modern VLSI technology provide the best means for achieving the goal of real-time signal processing and sufficient computational speed to support the ongoing interaction of a patient with the environment. Finally, there is the practical consideration of integration of the prosthetic system with the patient, i.e., it must be miniaturized sufficiently so it can be carried on board easily.

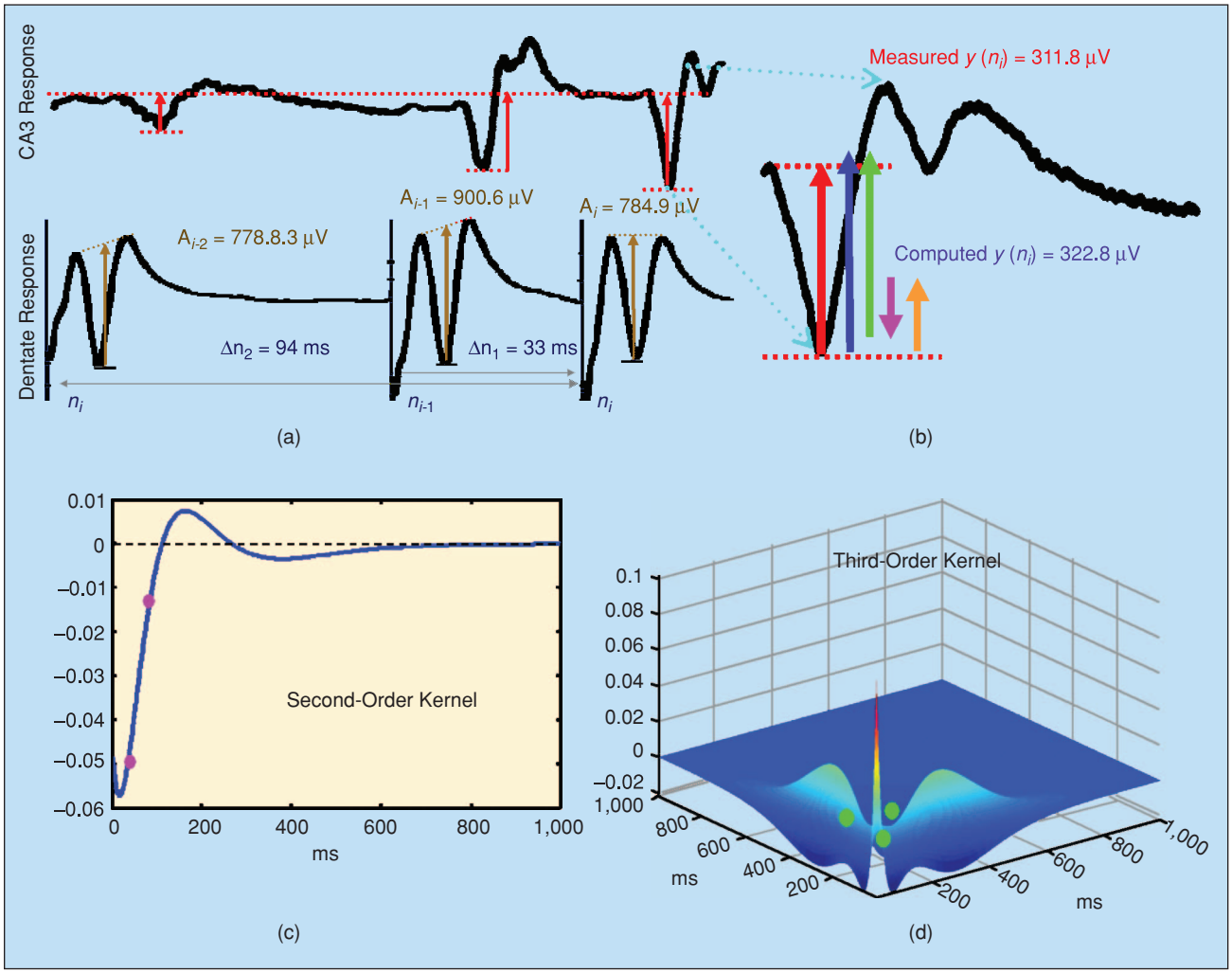

Fig. 6. An example of model prediction. (a) Top waveforms (measured CA3 output): three consecutive CA3 population spikes and the corresponding population spike amplitudes (red arrows); bottom waveforms (measured CA3 input): three consecutive dentate population spikes and the corresponding population spike amplitudes (brown). (b) Detail of the third population spike of the top waveforms in (a) recorded at CA3, its measured amplitude (positive, red arrow starting the peak of the population spike), and its model predicted counterpart (positive, blue arrow to the right of the measured amplitude), which is the sum of the component attributed to the first-order interactions (rightmost, positive, yellow arrow), the component attributed to the second-order interactions (negative, pink arrow to the left of the first-order term), and the component attributed to the third order interactions (positive, green arrow to the left of the second-order term). (c) Second-order kernel with the pink dots marking its weight to the contribution of the second-order interactions of the input population spike amplitudes shown on the bottom waveforms in (a). (d) Third-order kernel with the green dots marking its weight to the contribution of the third-order interactions among the input population spike amplitudes shown on the bottom waveforms in (a).

The system-on-a-chip we have developed for the hippocampal CA3 prosthesis, as depicted in Figure 8, accepts analog signals from the hippocampal dentate region (DG), buffers and amplifies the signals, and then performs an analog-to-digital conversion (ADC). The sequence of processing is controlled by a finite state machine (FSM), and automatic gain control circuitry adjusts the amplitude of the input signal. Once the signals are in binary form, other circuitry identifies and calculates the amplitude of the population spike ("Spike Detector" in Figure 8) and transmits the result to the circuitry that performs the nonlinear modeling function ("Polynomial Update" and "Response Generator" in Figure 8). Each digital nonlinear response prediction is delayed by a millisecond time period appropriate to dentate-to-CA3 propagation and then converted to a biphasic representation compatible with electrical stimulation of neuronal tissue (pulse-to-biphasic). The result is digital-to-analog conversion (DAC) and is transmitted to the biological tissue through a conformal multisite electrode array, described in the following section.

The real-time population spike amplitude identification and measurement is performed in the digital domain. Digital circuitry implemented on a field-programmable gate array (FPGA) is used to determine the population spike amplitude by a process of filtering, differentiation, and intelligent integration. The algorithm for real-time population spike extraction was written in C language. As described previously, nonlinearities of the hippocampal system are expressed as Volterra kernels. Each kernel is expressed as a summation of basis functions, which are chosen to be generalized Laguerre functions. Laguerre functions can be evaluated indirectly using a recursive tableau. Recursion is desirable for hardware implementation for several reasons. First, only one time step of memory is required; we can overwrite each memory location as a stale result that is no longer needed. Second, the operating speed of the circuit can be greatly reduced; only values required for the current time step must be calculated. Finally, the calculation never changes; hardware required for direct computation is much less complicated than a full programmable processor. The three cases of the calculation (initialization or time-step zero, polynomial order zero, and all others) are handled by multiplexing the boundary values into the circuit. The logic for the CA3 response calculation can be implemented in approximately 20,000 gates, a small fraction of an FPGA on a commercial board available from Dini Group in San Diego, California. To ensure real-time response, on every sample the state of the Laguerre polynomials must be updated, the presence of a CA3 population spike detected, and a response generated if a spike is detected. The numerical accuracy required for the recurrent computation of the Laguerre polynomials used as the basis function in the mathematical model was studied thoroughly. It was determined that a 20 b signed arithmetic would produce stable and accurate results over a recursion of 1,000 iterations. Figure 9 shows, for several inputs of a random impulse train applied to the perforant path, results of the FPGA-based CA3 model prediction compared to biological CA3 responses recorded from a hip-

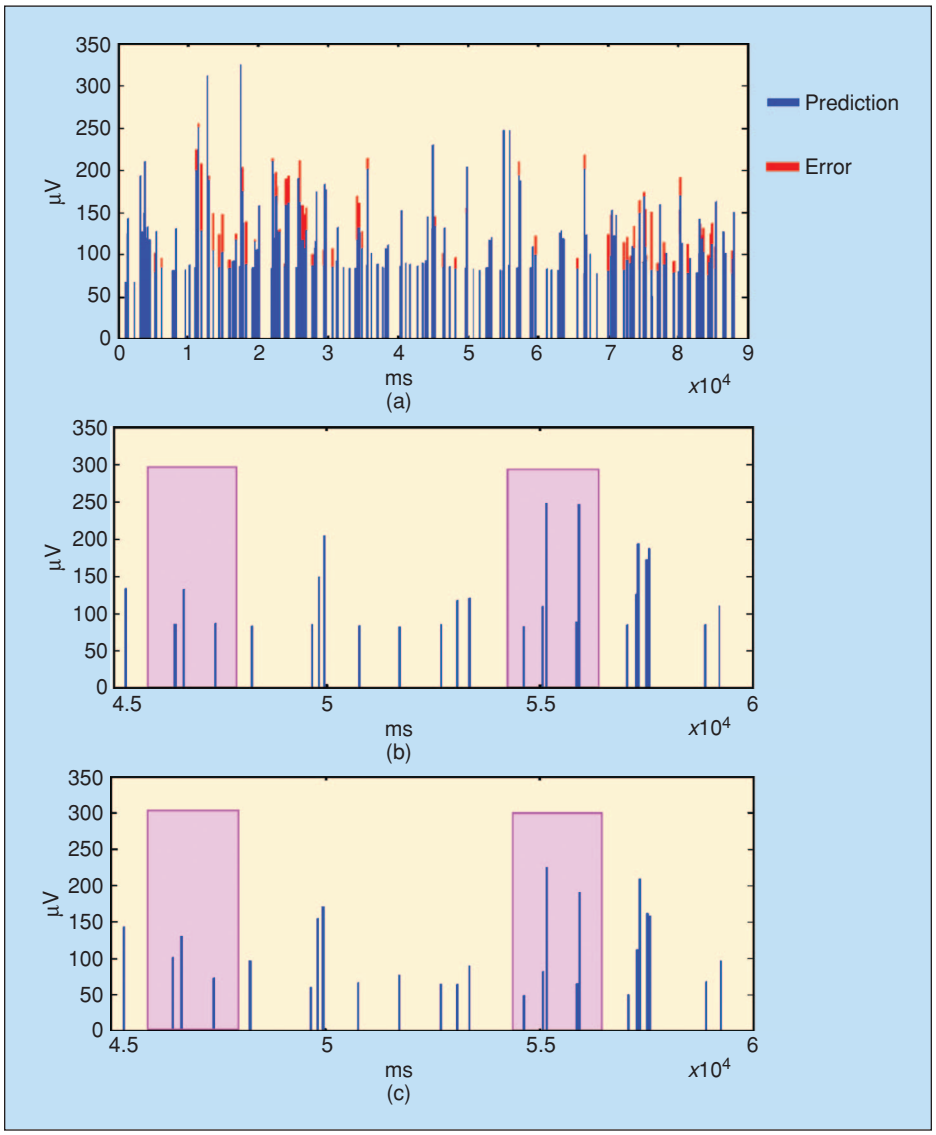

Fig. 7. CA3 model prediction (NMSE 5 8.21%): (a) Predicted population spike amplitudes (blue) and their differences from the corresponding measured population spike amplitudes (red); (b) a segment of the CA3 model prediction; and (c) the corresponding segment of the measured CA3 population spike amplitudes. The shaded rectangles highlight two areas for comparison between model predicted values and recorded values.

pocampal slice. It is evident that the correspondence between the hardware model and the biological system is high.

C programs for both population spike identification/measurement and nonlinear I/O modeling were converted to VHSIC hardware description language (VHDL) code; the VHDL code then was used to program the FPGA. This is a common and convienent strategy to converge on a VLSI implementation; the FPGA system provides a flexible, programmable environment for optimizing the desired functionalities in terms of a VHDL code, and the VHDL code is readily translated into VLSI design, minimizing the risk associated with developing a microchip device.

Conformal Multisite Electrode Arrays for Interfacing the Biomimetic Model of CA3 with Hippocampal Tissue

A biomimetic device for central brain regions must interact bidirectionally with the undamaged brain to support cognitive function and influence behavior. One of the indisputable characteristics of the mammalian brain is that anatomical connections between multiple neurons in one brain region and multiple neurons in a second brain region are not random—there is typically an identifiable topography in which neurons from one subregion of a given brain region project primarily to a localized subset of neurons in the target structure. Moreover, virtually all brain areas have region-specific cytoarchitectures, e.g., varying degrees of cellular and/or dendritic layering and geometries of curvature within which topographical connections are embedded. As a consequence of these considerations, bidirectional communication between a biomimetic device and the brain must be accomplished with one or more multisite electrode arrays, with the spatial distribution and density of recording/stimulating electrodes designed to match (be conformal with) the cytoarchitecture and topography-density of the brain regions providing the inputs and outputs of the device.

Two specific types of conformal multielectrode arrays have been implemented: 1) a multisite stimulation/recording multielectrode array capable of sampling the entire trisynaptic pathway, including the dentate gyrus, CA1, and CA3 regions of rat hippocampus (Trisynaptic cMEAs), and 2) a similar stimulation/recording multielectrode array capable of stimulating at the input to the dentate, recording the output from the dentate, interfacing with an external electronic or computer system capable of simulating the nonlinear I/O characteristics of the CA3 hippocampal region, stimulating at the input to CA1, recording the output from CA1, and interfacing once again with an external electronic or computer system (CA3 Replacement cMEAs). CA3 replacement demonstration experiments to date have been based on both computer and FPGA interfaces, pointing toward full integration with an application-specific integrated circuit (ASIC) implemented in a silicon-based VLSI circuit.

The Trisynaptic cMEA design, as shown in Figure 10(a), includes nine sets of seven linearly spaced 28-μm-diameter

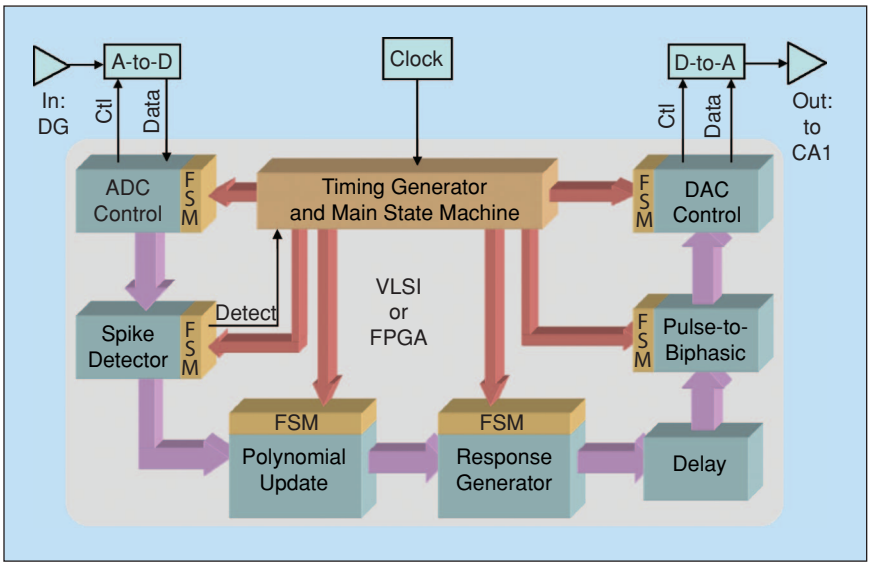

Fig. 8. A top-level system diagram showing the major functional blocks and the signal flow, including the relationship of the real-time spike detection, the response generator, and the output waveform generator, which are all in the digital domain.

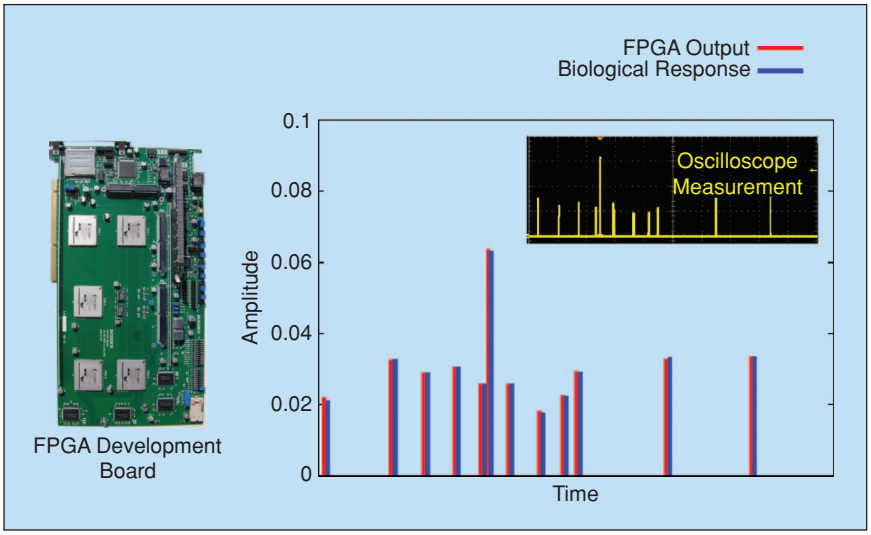

Fig. 9. A comparison of FPGA-based nonlinear model predictions of hippocampal CA3 output with biological CA3 output as a function of dentate population spike input for a segment of random impulse train stimulation of perforant path. Predicted (red bars) and electrophysiologically recorded CA3 population spike amplitudes (blue bars) are shown for a segment of random interval train stimulation. Recorded dentate population spike amplitudes for impulses within the random interval train were used as model input.

pads with a 50-μm center-to-center spacing, each set spanning one of the key input/output regions of the DG, CA3, and CA1 regions of rat hippocampus, thereby allowing for a complete diagnostic assessment of the nonlinear dynamics of the trisynaptic hippocampal circuitry. The CA3 Replacement cMEA design, as shown in Figure 10(b), includes two different circular pad sizes: 1) 28-μm diameter pads with a 50-μm center-to-center spacing are grouped in series to form sets of stimulating pads in dentate gyrus (three at a time) and CA1 (two at a time), and 2) 36-μm diameter pads also with a 50-μm center-to-center spacing are used for recording in DG, CA3, and CA1. By grouping sets of stimulating pads in series, we are able to achieve significantly larger pad surface areas and correspondingly larger total stimulating currents than are achievable with single pads while still maintaining essential conformality to cytoarchitecturally relevant features. These stimulating pads have been placed only in DG and CA1 in order to interface with the FPGA/VLSI hardware that replaces the CA3 region entirely and to thereby support the envisioned CA3 replacement experiment protocol. These conformal multielectrode arrays have provided a durable electrical interface between the neural tissue and the FPGA/VLSI hardware in initial CA3 replacement experiments, as described in more detail elsewhere in this article.

The general microfabrication procedure employed for these cMEAs is as follows. A set of indium tin oxide (ITO) electrical leads is defined on an ITO-coated glass substrate of dimensions 49 mm $\times$ 49 mm $\times$ 1.1 mm by the first photomask exposure and subsequent acid-bath etching. A silicon nitride insulation layer is then deposited by means of plasma-enhanced chemical vapor deposition (PECVD). This layer electrically insulates individual ITO lines from each other and from the saline solution that the cMEA will be exposed to during acute slice testing. A second photomask is then used to define the vias that will form the conformal metal (Cr/Au) electrode tips. The Cr/Au metal layer is deposited by electron-beam evaporation. After deposition of a second insulating layer composed of SU-8 photoresist, a final photolithographic exposure is performed to pattern vias through the insulation layer to the previously deposited gold electrodes. The thick (1.5 μm) epoxy-based SU-8 photoresist provides for decreased shunt capacitance of the cMEA as a whole, thereby enabling higher amplitude neural recordings. The array pinout includes 60 signal channels and is designed to be compatible with the multichannel systems MEA-60 apparatus.

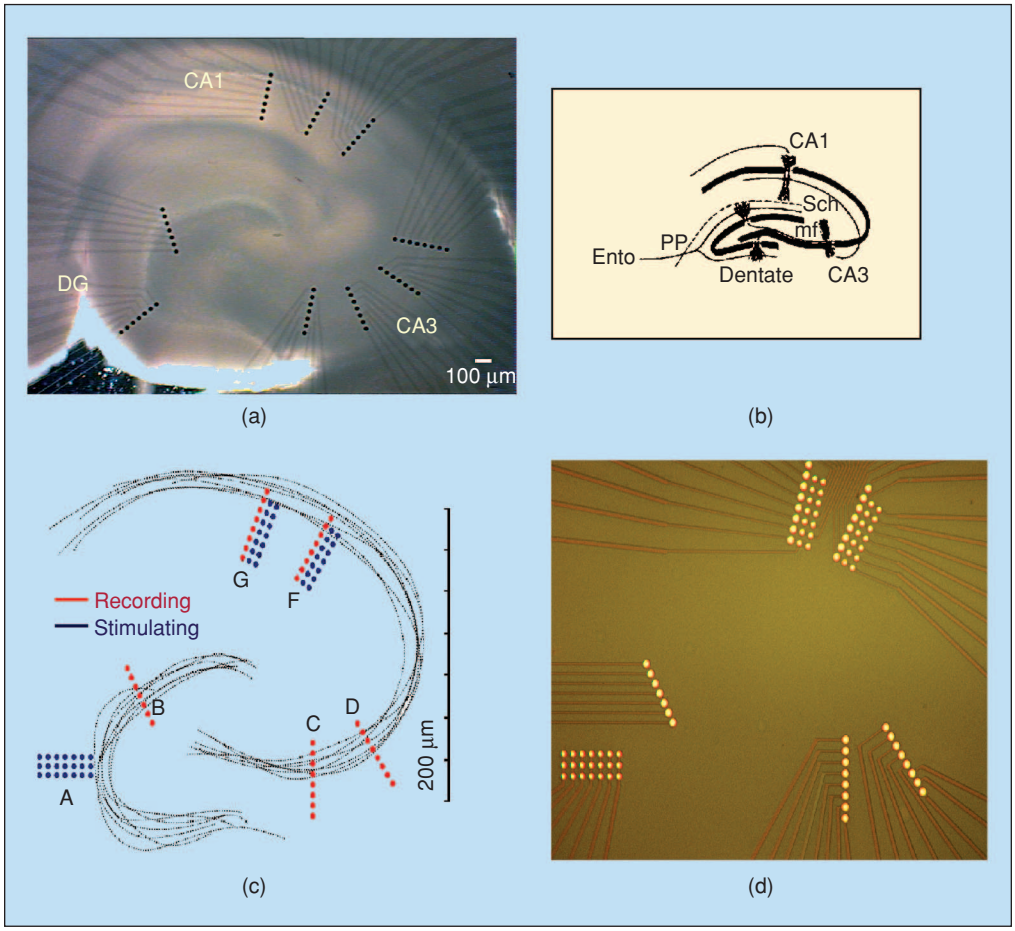

Fig. 10. (a) Optical photomicrograph of a cMEA incorporating the trisynaptic electrode pad layout that is proximity-coupled to a rat hippocampal slice. The nine sets of seven linearly-spaced 28-μm diameter pads conform to the DG, CA3, and CA1 regions. (b) A diagram of hippocampal cell regions. (c) Optical photomicrograph of the central region of a new conformal multielectrode array specifically designed for CA3 replacement demonstration. Stimulating and recording electrodes are arranged in both the DG and CA1 regions, while two sets of recording electrodes are provided in the CA3 region for prereplacement characterization.

System Integration: Restoration of Hippocampal Circuit Dynamics with the CA3 Prosthesis

Recall that the goal of this multidisciplinary effort is to achieve the Stage 1 prosthetic system for the hippocampal slice by integrating the components described above. More specifically, we seek to functionally replace the biological CA3 subregion of the hippocampal slice with an FPGA/VLSI-based model of the nonlinear dynamics of CA3, such that the propagation of temporal patterns of activity from dentate$\rightarrow$VLSI model$\rightarrow$CA1 reproduces that observed experimentally in the biological dentate$\rightarrow$CA3$\rightarrow$CA1 circuit. We have successfully performed the first integration of an FPGA-based nonlinear model of the CA3 hippocampal region with the hippocampal

slice, by interconnecting the FPGA and the living slice through a conformal, planar, multisite electrode array. We have succeeded in supporting the real-time communication of stimulation-induced responses of dentate granule cells from the slice to the FPGA, generation of CA3-like outputs from the FPGA device, FPGA-triggered stimulation of CA1, and recording of electrophysiological output from CA1.

The preparation we are using to test our Stage 1 prosthetic system is a hippocampal slice with severed CA3 afferents [the hippocampal slice is shown in Figure 11(a); the transection cannot be seen visually]. Electrical stimulation of inputs to the dentate gyrus still evokes excitatory responses from dentate granule cells in this preparation, but excitation cannot propagate through the remainder of the trisynaptic pathway, i.e., to CA3 and from CA3 to CA1. To reinstate the function of CA3, and thus reinstate propagation through the trisynaptic, we have interconnected our FPGA model of CA3 through the specially designed, conformal multisite electrode array (black dots in the slice photomicrograph) described in the previous section, which allows recording electrical activity from and stimulating electrical in the slice.

A demonstration of the integration of all components of our hippocampal slice prosthesis is shown in Figure 11. In this example, we have used only a subset of possible stimulation patterns and, more specifically, four-impulse trains with variable interimpulse intervals as inputs to a transected slice. Although limited in terms of number of impulses, the interimpulse intervals were chosen to evoke large-magnitude nonlinearities in the responses of dentate granule cells. Thus, stimulation of inputs to the dentate with a variable-interval four-impulse train [Figure 11(a)] generates variable-amplitude output from dentate granule cells [Figure 11(b)]. The output is recorded by the multisite array and transmitted to the FPGA model of CA3 [Figure 11(c)]. The FPGA model A/D converts the extracellular population waveform, identifies the population spike component of that waveform, and calculates its amplitude. Based on the amplitude and history of interimpulse intervals, the FPGA-based nonlinear model of CA3 computes the appropriate CA3 output in terms of biphasic stimulation pulses [Figure 11(d)] (the magnitude of which are equivalent to the population spike amplitude that would have been generated in the CA3 by that particular output). The biphasic output pulses generated by the FPGA are transmitted through the multisite array and used to electrically stimulate inputs to CA1 [Figure 11(e)]. The resulting variable-amplitude output [population excitatory postsynaptic potential (EPSP)] is recorded from CA1 [Figure 11(f)], demonstrating the functional reinstatement of

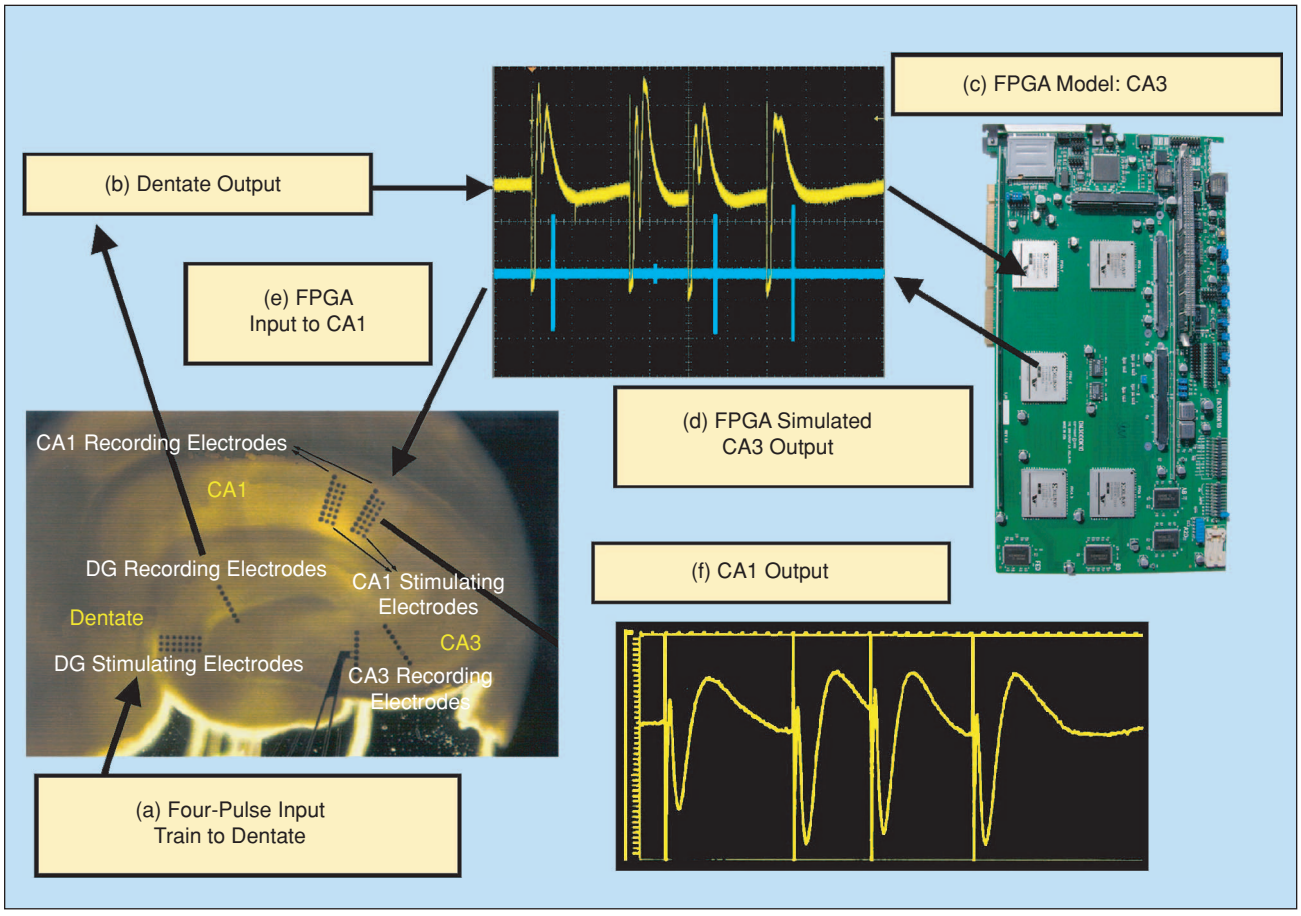

Fig. 11. System integration of an FPGA-based nonlinear model of the CA3 hippocampal region with a hippocampal slice in which the output from the dentate gyrus (mossy fibers in the hilus) have been transected, thus eliminating the normal propagation of activity from dentate→CA3→CA1. The FPGA-based model bidirectionally communicates with the living slice through a conformal, planar, multisite electrode array. This system supports real-time communication of stimulation-induced responses of dentate granule cells from the slice to the FPGA, generation of CA3-like outputs from the FPGA device, FPGA-triggered stimulation of CA1, and recording of electrophysiological output from CA1.

the dentate→CA3→CA1 circuit. These results demonstrate that the various components we have proposed for our prosthesis can be developed and effectively integrated into a working system.

We are currently in the process of fully evaluating the output generated in the CA1 region by our CA3 prosthesis system, i.e., comparing CA1 output in response to the FPGA model of CA3 with the output of CA1 in response to the biological CA3. For these tests, we are using random impulse train stimulation of the perforant path (rather than four-impulse trains with variable interimpulse intervals as described for Figure 11). Examples of results from two random impulse train experiments are shown in Figure 12. Each chart illustrates results from one experiment: amplitudes of population EPSPs recorded from the CA1 region are shown as a function of 50 impulses chosen from among 2,400 impulses of the random trains (1,200 administered before transecting inputs to CA3 and 1,200 administered after transection). Time intervals between impulses are not represented in the figures; only input event number (sequence of sample impulses) is shown to collapse the *x*-axis. Data for the intact slice (CA1 trisynaptic) is shown in pink boxes; data for the hybrid slice with the substituted FPGA model of CA3 (CA1 replacement) is shown in dark blue diamonds. For what is a wide range of intervals captured in this 50-impulse sequence, and what is a three- to fivefold difference in population EPSP amplitude, CA1 output from the hybrid slice matches extremely well the CA1 output from the intact slice. In particular, those intervals that generate large amplitude CA1 population EPSPs in the intact slice also are the only intervals that are associated with the large amplitude CA1 responses in the hybrid slice. The biomimetic device does not generate unexpected or abberant dysfunctional, large amplitude CA1 responses. Importantly, intervals that lead to smaller-scale fluctuations in CA1 output of the CA1 slice also emerge in the hybrid system, i.e., subtle aspects of hippocampal trisynaptic circuit dynamics also are are faithfully reproduced. Further quantification studies are in progress.

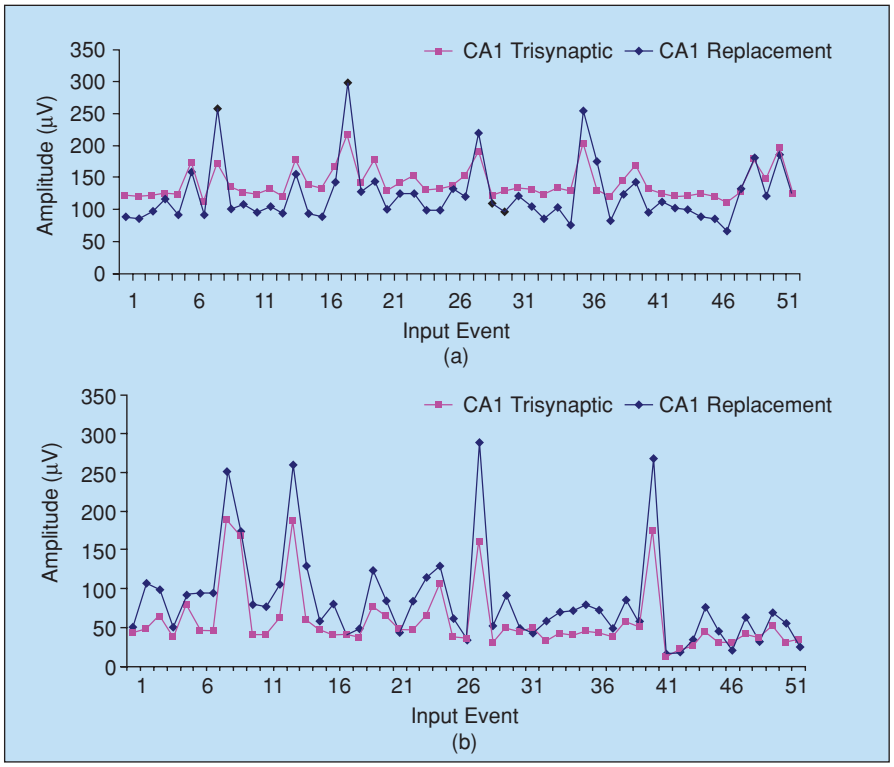

Fig. 12. A comparison of hippocampal CA1 output in response to the FPGA model of CA3 with the output of CA1 in response to the biological CA3. Examples of results from two random impulse train experiments are shown in the two charts: amplitudes of population EPSPs recorded from the CA1 region are shown as a function of 50 impulses chosen from among 2,400 impulses of the random trains (1,200 administered before transecting inputs to CA3; 1,200 administered after transection). Time intervals between impulses are not represented in the figure; only the Input Event number (sequence of sample impulses) is shown to "collapse" the *x*-axis. Data for the intact slice (CA1 Trisynaptic) are shown in pink boxes; data for the "hybrid" slice with the substituted FPGA model of CA3 (CA1 Replacement) are shown in blue diamonds. For what is a wide range of intervals captured in this 50-impulse sequence, and what is a three- to fivefold difference in population EPSP amplitude, note that CA1 output from the "hybrid" slice matches extremely well the CA1 output from the intact slice.

Extension to the Hippocampus of the Behaving Animal

The research described here represents the first step in developing a neural prosthesis for the hippocampus of the behaving animal, and ultimately of the human, to restore memory function after damage. In animals (and humans) performing learned behaviors, memory-related information is coded in a distributed manner among a population (or ensemble) of neurons, each subpopulation firing at different times and with different patterns in relation to environmental and behavioral cues [39]–[41]. Thus, extending the approach described here to the behaving animal will require

- multiple input-multiple output models to represent the nonlinear dynamics of each of the different subpopulations of the ensemble
- a more complex VLSI device design (perhaps involving a multichip module) to implement the multiple input-multiple output model
- vertically oriented, conformal, multisite electrode arrays capable of penetrating into the hippocampus from the surface of the brain to record/stimulate target regions
- development and application of packaging technologies to integrate VLSI and electrode sensing/acuating functions
- surface patterning of novel chemistries to increase biocompatibility of microfabricated materials/ devices.

Progress on these critial fronts is currently proceeding [42]–[45]. Extending the biomimetic cortical prosthesis approach demonstrated here to the behaving animal/human also will require dealing with issues that we have yet to address, namely,

context-dependence of hippocampal nonlinearities, i.e., the influence of stress, diurnal cycles, and learning-related alterations of hippocampal nonlinearities. An additional challenge will be accounting for the well-established reactivity of the hippocampal circuitry to damage and injury. Incorporating these physiological factors will require significant elaborations of the current model, the means for alteration of model parameters as a function of environmental setting and experience as well as the possibility of dynamic reconfiguration of the spatial distribution of multisite electrode array elements.

Acknowledgments

This research was supported by the Brain Restoration Foundation, DARPA DSO (HAND Program), the National Science Foundation Engineering Research Center (ERC) in Biomimetic Microelectronics Systems, NSF BITS Program, the Office of Naval Research (ONR) Adaptive Neural Systems Program, the ONR AINS Program, and the National Institutes of Health/National Institute of Biomedical Imaging and Bioengineering (NIBIB) University of Southern California Biomedical Simulations Resource.

Theodore W. Berger is a professor of biomedical engineering and neurobiology and the director of the Center for Neural Engineering at the University of Southern California (USC). He received his Ph.D. from Harvard University in 1976, for which he received the James McKeen Cattell Award from the New York Academy of Sciences. He conducted postdoctoral research at the University of California, Irvine, and was an Alfred P. Sloan Foundation Fellow at the Salk Institute. He joined the Departments of Neuroscience and Psychiatry at the University of Pittsburgh, being to the level of full professor in 1987. During that time, he received a McKnight Foundation Scholar Award, twice received a National Institute of Mental Health (NIMH) Research Scientist Development Award, and was elected a Fellow of the American Association for the Advancement of Science. Since 1992, he has been professor of biomedical engineering and neurobiology at USC. He has received an NIMH Senior Scientist Award, was awarded the Lockheed Senior Research Award, and was elected a fellow of the American Institute for Medical and Biological Engineering. He became director of the Center for Neural Engineering in 1997, an organization which helps to unite the numerous USC faculty with cross-disciplinary interests in neuroscience, engineering, and medicine. He has published more than 150 journal articles and book chapters.

Ashish Ahuja received a B.S. degree in applied physics and an M.S. degree in electrical engineering from Columbia University in 1999 and 2002, respectively. He worked for two years in the condensed matter physics department and fiber optics devices department at Bell Laboratories. In 2002, he came to the University of Southern California to work toward a Ph.D. in the Electrical Engineering-Electrophysics department.

Spiros H. Courellis received his diploma in electrical engineering from the Aristotle University of Thessaloniki, Greece, in 1985, his M.S. in electrical engineering from the California Institute of Technology, Pasadena, in 1986, and his Ph.D. in electrical engineering from the University of Southern California, Los Angeles, California, in 1992. He was a research associate with the Biomedical Engineering Department at the University of Southern California, from 1993–2004. During that period of time, he also held industrial appointments research and development, education, and leadership. Since 2004, he has been a research assistant professor of biomedical engineering at the University of Southern California. His main research interests are in the areas of on nonlinear dynamic modeling of spatiotemporal multi-input/multi-output neural information processing systems, biologically inspired information fusion systems, biosensors, neural computation and memory, and distributed implantable secure medical devices. He is a Member of IEEE, ACM, and the Society for Neuroscience.

Samuel A. Deadwyler is a professor of physiology and pharmacology, Department of Physiology and Pharmacology, Wake Forest University School of Medicine (WFUSM). He received his Ph.D. in 1970 from the State University of New York, Stony Brook. He conducted postdoctoral research at the University of California, Irvine from 1971–1977 and became an assistant professor of physiology and pharmacology at WFUSM in 1977. He was promoted to professor in 1984 and became vice chair in 1989. He has been funded by the National Institutes of Health (NIH) continuously since 1974, is the ongoing recipient of a NIH Senior Research Scientist award, which began in 1987, and a NIDA MERIT awardee from 1990–2000. He has served on the editorial board for the *Journal of Neuroscience* since 1996 and was a reviewing editor of that journal from 2001–2005. He also sits on the editorial board of the journal *Hippocampus*. He has been an invited Grass Foundation lecturer on four different occasions. He is past president of the International Cannabinoid Research Society and currently on the Board of Directors of the College on Problems of Drug Dependence. He has served on many national committees, including NIH review and policy making bodies as well as private industrial advisory panels. He has more than 150 publications including journal articles, chapters, and books relating to neural mechanisms of learning and memory as well as cellular neurophysiological investigation of drug actions. His research interests include mechanisms of information encoding in neuronal populations, relationship between neuronal codes and behavioral performance, mechanisms of enhancement of short-term memory in relation to neural codes generated in the hippocampus and with respect to drugs that enhance synaptic activity, processes underlying the neuronal representation of reward and actions of abused drugs, interactions between brain functions during informations processing and modification of behavioral performance by factors such as sleep deprivation, and development of wireless feedback control of performance by altering task contingencies in relation to neural encoding of task-relevant information.

Gopal Erinjippurath received his bachelor's degree in electronics and communication engineering from the TKM College of Engineering, University of Kerala, India, in 2003 and his M.S. degree in electrical engineering from the University of Southern California, Los Angeles in 2005. Since December 2003, he has been a research assistant at the Biomedical Engineering Department, University of Southern California, Los Angeles. His areas of interest are nonlinear data analysis and modeling, multimedia, and adaptive signal processing.

Gregory A. Gerhardt received his Ph.D. in chemistry in 1983 from the University of Kansas. He received postdoctoral training in pharmacology, neuroscience, and psychiatry at the University of Colorado Health Sciences Center in Denver from 1983–1985. He is currently a professor in the Anatomy and Neurobiology, Neurology, and Psychiatry departments at the University of Kentucky (UK) Chandler Medical Center, Lexington, Kentucky. He is the director of the Morris K. Udall Parkinson's Disease Research Center of Excellence and director of the Center for Sensor Technology (CenSeT), both at UK. He is also the editor in chief, Americas and Australasia, of the *Journal of Neuroscience Methods*. He holds one U.S. patent and several patent applications are in progress. He has authored or coauthored more than 240 peer-reviewed papers and book chapters and more than 300 scientific abstracts. His laboratory focuses on growth factors and their effects on the central nervous system (CNS), as applied to studies of normal aging and repair of the brain in Parkinson's disease. In addition, his laboratory develops microelectrode recording methods to study the dynamics of neurotransmitter release in the CNS and to develop neuronal interface devices. He has received numerous awards, including a Research Scientist Development Award (RSDA Level II from NIMH).

Ghassan Gholmieh received his bachelor of science (chemistry) and his medical diploma from the American University of Beirut in 1994 and 1998, respectively. He completed an internship in internal medicine at the University of Southern California (USC) in July 2002. He then defended his dissertation leading to a Ph.D. in biomedical engineering at USC in December 2002. He is currently a research assistant professor at USC and is working with Dr. Theodore Berger on the cortical prosthesis project.

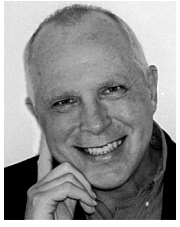

John J. Granacki received a B.A. from Rutgers University, New Jersey, an M.S. in physics from Drexel University, Pennsylvania, and an engineer and Ph.D. in electrical engineering from the University of Southern California. He is currently the director of the Advanced Systems Division at the University of Southern California's Information Sciences Institute, research associate professor in the Department of Electrical Engineering Systems and the Department of Biomedical Engineering. He is the leader of the mixed-signal systems on a chip thrust in the National Science Foundation Biomimetic Microelectronics Engineering Research Center. His research interests include high performance embedded computing systems, multiprocessor system-on-chip architectures, biologically inspired computing, and advanced architectures for cognitive computing. He is a Member of the IEEE Computer Society and Circuit and Systems Society, the ACM, and the Society for Neuroscience.

Robert Hampson is an associate professor at Wake Forest University School of Medicine in the Department of Physiology and Pharmacology. He received his Ph.D. degree from Wake Forest University in 1988 in physiology. He was a postdoctoral fellow and assistant professor at that institution from 1989–1998 when he was promoted to the rank of associate professor. He is a past member of the IFCN-7 National Institutes of Health (NIH) review panel and has served as an ad hoc member of other review panels for NIH. His main interests are in computer analysis and modeling of neural encoding in hippocampus and other related structures, as well as alterations of that encoding by drug abuse. He has published extensively in the areas of cannabinoid effects on behavior and electrophysiology, and the correlation of behavior with multineuron activity patterns, particularly applying linear discriminant analysis to neural data to decipher population encoding and representation.

Min Chi Hsiao received his B.S. and M.S. degrees in biomedical engineering from Chung Yuan Christian University, Chung-Li, Taiwan, in 1998 and 2000, respectively. From 2002–2003, he worked as a research assistant in the neural regeneration lab, Taipei Veteran General Hospital, Taiwan. He is currently pursuing a Ph.D. degree in biomedical engineering at the University of Southern California. His research interests include electrophysiology, neuroanatomy, and animal experimentation.

Jeffrey LaCoss is a project leader in the University of Southern California ISI Advanced Systems. His current research is in three principal areas: very high performance processing for embedded platforms, low-power hardware models for brain replacement and augmentation, and cognitive systems architectures inspired by neural principals. He is a Member of IEEE Computer Society and the Society for Neuroscience.

Vasilis Z. Marmarelis received his diploma in electrical engineering and mechanical engineering from the National Technical University of Athens in 1972 and the M.S. and Ph.D. degrees in engineering science (information science and bioinformation systems) from the California Institute of Technology, Pasadena, in 1973 and 1976, respectively. After two years of

postdoctoral work at the California Institute of Technology, he joined the faculty of biomedical and electrical engineering at the University of Southern California, Los Angeles, where he is currently Professor and Director of the Biomedical Simulations Resource, funded by the National Institutes of Health since 1985 and dedicated to modeling/simulation studies of biomedical systems. He served as Chairman of the Biomedical Engineering Department from 1990–1996. His main research interests are in the areas of nonlinear and nonstationary system identification and modeling, with applications to biology, medicine, and engineering systems. Other interests include spatiotemporal and nonlinear/nonstationary signal processing, high-resolution 3-D ultrasonic imaging, and analysis of neural systems and networks with regard to information processing. He is coauthor of the book *Analysis of Physiological System: The White Noise Approach* (New York: Plenum, 1978; Russian translation: Moscow, Mir Press, 1981; Chinese translation: Academy of Sciences Press, Beijing, 1990), editor of three volumes on advanced methods of physiological system modeling (1987, 1989, and 1994) and author of the book *Nonlinear Dynamic Modeling of Physiological Systems* (2004). He has published more than 100 papers and book chapters in the area of system and signal analysis. He is a Fellow of the IEEE and of the American Institute for Medical and Biological Engineering.

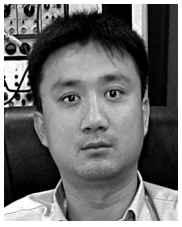

Dong Song received his B.S. degree in biophysics from the University of Science and Technology of China in 1994 and his Ph.D. degree in biomedical engineering from the University of Southern California (USC) in 2003. Since 2004, he has been working as a postdoctoral fellow in the Center for Neural Engineering, USC. His main research interests include electrophysiology of the hippocampus, nonlinear systems analysis of the nervous system, and the development of a combined parametric/nonparametric modeling approach.

Armand R. Tanguay, Jr. is a professor of electrical engineering, materials science, and biomedical engineering at the University of Southern California. He received a B.S. degree in physics (Cum Laude) from the California Institute of Technology in 1971, and M.S., M.Phil., and Ph.D. degrees in engineering and applied science from Yale University in 1972, 1975, and 1977, respectively. He is a founding member of the Center for Photonic Technology, serving in the past as both deputy director and director. He was a founding member of the Integrated Media Systems Center, a National Science Foundation (NSF) Engineering Research Center in multimedia and creative technologies, serving as deputy director and associate director for research from 1995–1997, and is also a founding member of the Biomimetic MicroElectronics Systems Center, an NSF Engineering Research Center in neural prosthetic devices. He has further served as director of the Center for Neural Engineering, associate director for research of the Signal and Image Processing Institute, and is a member of both the Neuroscience Graduate Program and the Neural, Informational, and Behavioral Sciences Program at USC. His research interests and experience include the crystal growth and characterization of optical and optoelectronic materials; dielectric and optical thin film physics; thin film deposition technology and characterization; device processing by ion beam milling and etching techniques; electronic/photonic packaging including multichip module integration by flip-chip bonding; physical optics; the physics and technology of electrooptic, optoelectronic, and integrated optical devices (including spatial light modulators, photorefractive volume holographic optical elements, diffractive optical elements, and advanced integrated optical signal processors); photonic implementations of neural networks; smart cameras (including adaptive nonlinear dynamic range compression and color constancy); surgically implantable intraocular cameras and multielectrode arrays for retinal prostheses; immersive panoramic cameras; three-dimensional (3-D) visualization and full-volume 3-D displays; chaos in neural networks; two-dimensional (2-D) and 3-D conformal multielectrode neural probes and neural unit array prostheses for the brain; hybrid biological/electronic/photonic computational modules; and the fundamental and technological limitations of optical information processing and computing. His current research programs are highly interdisciplinary in nature and include the development of hybrid electronic/photonic multichip modules for vision applications; the design, fabrication, and testing of an intraocular camera to be used in conjunction with advanced conformal multielectrode arrays to form a retinal prosthesis for blindness induced by retinitis pigmentosa and macular degeneration; the use of human psychophysical techniques to develop optimal image acquisition and stimulation protocols for retinal prosthetic devices with limited numbers of microstimulator electrodes; the study of lateral brightness and chromatic adaptation in the human visual system; and the search for the fundamental origins of layering throughout the human visual and cortical systems. He is a Fellow of the Optical Society of America (OSA) and the American Association for the Advancement of Science (AAAS), and has received the Yale University Harding Bliss Prize, the USC Faculty Service Award, and the Rudolph Kingslake Medal and Prize of the Society of Photo-Optical Instrumentation Engineers (SPIE–The International Society for Optical Engineering). He has served as an elected Faculty Fellow of the Center for Excellence in Teaching at the University of Southern California from 2001–2005 and was named a Distinguished Faculty Fellow in May 2005. In addition, he was presented with a Teacher of the Year award in 2002 by the USC Latter Day Saint Student Association.

Address for Correspondence: Theodore W. Berger, Ph.D., Biomedical Engineering, DRB140/MC111, USC Viterbi School of Engineering, University of Southern California, Los Angeles, CA 90089 USA. Phone: +1 213 740 9360. Fax: +1 213 821 2368. E-mail: berger@bmsrs.usc.edu.

References

[1] T.W. Berger and D.L. Glanzman, *Toward Replacement Parts for the Brain: Implantable Biomimetic Electronics as the Next Era in Neural Prostheses*. Cambridge, MA: MIT Press, to be published.

[2] M.S. Humayun, E. de Juan Jr., J.D. Weiland, G. Dagnelie, S. Katona, R.J. Greenberg, and S. Suzuki, "Pattern electrical stimulation of the human retina," *Vision Res.*, to be published.

[3] G.E. Loeb, "Cochlear prosthetics," *Ann. Rev. Neurosci.*, vol. 13, pp. 357–371, 1990.

[4] R.A. Normann, D.J. Warren, J. Ammermuller, E. Fernandez, and S. Guillory, "High-resolution spatio-temporal mapping of visual pathways using multielectrode arrays," *Vision Res.*, vol. 41, no 10–11, pp. 1261–1275, 2001.

[5] G.E. Loeb, R.A. Peck, W.H. Moore, and K. Hood, "BION system for distributed neural prosthetic interfaces," *Med. Eng. Phys.*, vol. 23, no. 1, pp. 9–18, 2001.

[6] K.H. Mauritz and H.P. Peckham, "Restoration of grasping functions in quadriplegic patients by functional electrical stimulation (FES)," *Int. J. Rehab. Res.*, vol. 10, no. 4, suppl. 5, pp. 57–61, 1987.

[7] J.P. Donoghue, "Connecting cortex to machines: Recent advances in brain interfaces" *Nature Neurosci.*, vol. 5, suppl., pp. 1085–1088, 2002.

[8] M.A. Nicolelis, "Brain-machine interfaces to restore motor function and probe neural circuits," *Nature Revs. Neurosci.*, vol. 4, no. 5, pp. 417–422, 2003.

[9] K.V. Shenoy, D. Meeker, S. Cao, S.A. Kureshi, B. Pesaran, C.A. Buneo, A.P. Batista, P.P. Mitra, J.W. Burdick, and R.A. Andersen, "Neural prosthetic control signals from plan activity," *Neuroreport*, vol. 14, no. 4, pp. 591–596, 2003.

[10] T.W. Berger, M. Baudry, R.D. Brinton, J.-S. Liaw, V.Z. Marmarelis, Y. Park, B.J. Sheu, and A.R. Tanguay Jr., "Brain-implantable biomimetic electronics as the next era in neural prosthetics," *Proc. IEEE*, vol. 89, no. 7, pp. 993–1012, 2001.

[11] T.W. Berger, R.B. Brinton, V.Z. Marmarelis, B.J. Sheu, and A.R. Tanguay Jr., "VLSI implementations of biologically realistic hippocampal neural network models," in *Toward Replacement Parts for the Brain: Implantable Biomimetic Electronics as the Next Era in Neural Prosthetics,* T.W. Berger and D.L. Glanzman, Eds. Cambridge, MA: MIT Press, to be published.

[12] B. Milner, "Memory and the medial temporal regions of the brain," in *Biology of Memory,* K.H. Pribram and D.E. Broadbent, Eds. New York: Academic, 1970, pp. 29–50.

[13] L.R. Squire and S.M. Zola, "Episodic memory, semantic memory, and amnesia," *Hippocampus*, vol. 8, no. 3, pp. 205–211, 1998.

[14] T.W. Berger and J.L. Bassett, "System properties of the hippocampus," in *Learning and Memory: The Biological Substrates,* I. Gormezano and E.A. Wasserman, Eds. Hillsdale NJ: Lawrence Erlbaum, 1992, pp. 275–320.

[15] H. Eichenbaum, "The hippocampus and mechanisms of declarative memory," *Behav. Brain Res.*, vol. 103, no. 2, pp. 123–133, 1999.

[16] S. Gais and J. Born, "Declarative memory consolidation: mechanisms acting during human sleep," *Learn Mem.,* vol. 11, no. 6, pp. 679–685, 2004.

[17] J. O'Keefe and L. Nadel, *The Hippocampus as a Cognitive Map*. London, UK: Oxford Univ. Press, 1978.

[18] S.A. Deadwyler, T. Bunn, and R.E. Hampson, "Hippocampal ensemble activity during spatial delayed-nonmatch-to-sample performance in rats," *J. Neurosci.*, vol. 16, no. 1, pp. 354–372, 1996.

[19] P. Andersen, T.V. Bliss, T. Lomo, L.I. Olsen, and K.K. Skrede, "Lamellar organization of hippocampal excitatory pathways," *Acta Physiol. Scand.*, vol. 76, no. 1, pp. 4A5A, 1969.

[20] D.G. Amaral and M.P. Witterm, "The three-dimensional organization of the hippocampal formation: A review of anatomical data," *Neurosci.*, vol. 31, no. 3, pp. 571–591, 1989.

[21] T.W. Berger, T.P. Harty, X. Xie, G. Barrionuevo, and R.J. Sclabassi, "Modeling of neuronal networks through experimental decomposition," in *Proc. IEEE 34th Mid Symp. Cir. Sys.*, Monterey, CA, 1991, vol. 1, pp. 91–97.

[22] T.W. Berger, G. Chauvet, and R.J. Sclabassi, "A biologically based model of functional properties of the hippocampus," *Neural Netw.*, vol. 7, no. 6–7, pp. 1031–1064, 1994.

[23] S.S. Dalal, V.Z. Marmarelis, and T.W. Berger, "A nonlinear positive feedback model of glutamatergic synaptic transmission in dentate gyrus," in *Proc. 4th Joint Symp. Neural Computation*, California, 1997, vol. 7, pp. 68–75.

[24] Z. Wang, D. Song, and T.W. Berger, "Contribution of NMDA receptor channels to the expression of LTP in the hippocampal dentate gyrus," *Hippocampus*, vol. 12, no. 5, pp. 680–688, 2002.

[25] D. Song, Z. Wang, and T.W. Berger, "Contribution of T-type VDCCs to TEA-induced long-term synaptic modification in hippocampal CA1 and dentate gyrus," *Hippocampus*, vol. 12, no. 5, pp. 689–697, 2002.

[26] D. Song, Z. Wang, V.Z. Marmarelis, and T.W. Berger, "Nonparametric interpretation and validation of parametric models of short-term plasticity," in *Proc. IEEE EMBS Conf.*, Cancun, Mexico, 2003, pp. 1901–1904.

[27] G. Gholmieh, S.H. Courellis, D. Song, Z. Wang, V.Z. Marmarelis, T.W. Berger, "Characterization of short-term plasticity of the dentate gyrus-CA3 system using nonlinear systems analysis," in *Proc. IEEE EMBS Conf.*, Cancun, Mexico, 2003, pp. 1929–1932.

[28] A. Dimoka, S.H. Courellis, D. Song, V.Z. Marmarelis, and T.W. Berger, "Identification of lateral and medial perforant path using single- and dual-input random impulse train stimulation," in *Proc. IEEE EMBS Conf.*, Cancun, Mexico, 2003, pp. 1933–1936.

[29] R.J. Sclabassi, D.N. Krieger, and T.W. Berger, "A systems theoretic approach to the study of CNS function," *Ann. Biomed. Eng.* vol. 16, no. 1, pp. 17–34, 1988.

[30] R.J. Sclabassi, J.L. Eriksson, R. Port, G. Robinson, and T.W. Berger, "Nonlinear systems analysis of the hippocampal perforant path-dentate projection I. Theoretical and interpretational considerations," *J. Neurophysiol.*, vol. 60, no. 3, pp. 1066–1076, 1988.

[31] T.W. Berger, J.L. Eriksson, D.A. Ciarolla, and R.J. Sclabassi, "Nonlinear systems analysis of the hippocampal perforant path-dentate projection II. Effects of random train stimulation," *J. Neurophysiol.*, vol. 60, no. 3, pp. 1077–1094, 1988.

[32] T.W. Berger, J.L. Eriksson, D.A. Ciarolla, and R.J. Sclabassi, "Nonlinear systems analysis of the hippocampal perforant path-dentate projection III. Comparison of random train and paired impulse analyses," *J. Neurophysiol.*, vol. 60, no. 3, pp. 1095–1109, 1988.

[33] N. Wiener, *Nonlinear Problems in Random Theory*. New York: Wiley, 1958.

[34] V. Volterra, *Theory of Functions and of Integral and Integro-differential Equations*. New York: Dover Publications, 1930.

[35] P.Z. Marmarelis and V.Z. Marmarelis, *Analysis of Physiological Systems: The White-Noise Approach*. New York: Plenum Press, 1978.

[36] V.Z. Marmarelis, "Identification of nonlinear biological systems using Laguerre expansions of kernels," *Ann. Biomed. Eng.*, vol. 21, no. 6, pp. 573–589, 1993.

[37] K. Alataris, T.W. Berger, and V.Z. Marmarelis, "A novel network for nonlinear modeling of neural systems with arbitrary point-process inputs," *Neural Networks*, vol. 13, no. 2, pp. 255–266, 2000.

[38] T.W. Berger, J.J. Granacki, V.Z. Marmarelis, B.J. Sheu, and A.R. Tanguay Jr., "Brain-implantable biomimetic electronics as neural prosthetics," in *Proc. 1st Int. IEEE EMBS Conf. Neural Eng.*, Capri Island, Italy, 2003, pp. 108–111.

[39] T.W. Berger, P. Rinaldi, D.J. Weisz, and R.F. Thompson, "Single unit analysis of different hippocampal cell types during classical conditioning of the rabbit nictitating membrane response," *J. Neurophysiol.*, vol. 50, no. 5, pp. 1197–1219, 1983.

[40] M.L. Shapiro and H. Eichenbaum, "Hippocampus as a memory map: Synaptic plasticity and memory encoding by hippocampal neurons," *Hippocampus*, vol. 9, no. 4, pp. 365–384, 1999.

[41] R.E. Hampson, J.D. Simeral, and S.A. Deadwyler, "Distribution of spatial and nonspatial information in dorsal hippocampus," *Nature*, vol. 402, no. 6762, pp. 610–614, 1999.

[42] A.K. Ahuja, P. Nasiatka, D. Song, T.W. Berger, and A.R. Tanguay, "A biomimetic electronic prosthetic for hippocampus: Planar conformal multielectrode arrays for VLSI/hippocampal slice interface," in *Soc. Neurosci. Abstr.*, San Diego, CA, 2004, vol. 190.4.

[43] G.A. Gerhardt, P. Huettl, R.D. Brinton, S.A. Deadwyler, J.J. Granacki, R.E. Hampson, V.Z. Marmarelis, A.R. Tanguay, M.E. Thompson, and T.W. Berger, "A biomimetic electronic prosthetic for hippocampus: Conformal multisite platinum ceramic-based microarrays," in *Soc. Neurosci. Abstr.*, San Diego, CA, 2004, vol. 190.6.

[44] R.E. Hampson, S.H. Courellis, W. Davis, J.K. Konstantopoulos, T.W. Berger, and S.A. Deadwyler, "A biomimetic electronic prosthetic for hippocampus: Functional connectivity between hippocampal CA3 and CA1 neurons during behavior," in *Soc. Neurosci. Abstr.*, San Diego, CA, 2004, vol. 190.7.

[45] W. Soussou, C.M. Phipps, A. Bansal, M. Baudry, A. Madhukar, R.D. Brinton, T.W. Berger, and M.E. Thompson, "A biomimetic electronic prosthetic for hippocampus: Selective attachment of neurons and glia on biochemically modified electrode surfaces," in *Soc. Neurosci. Abstr.*, San Diego, CA, 2004, vol. 190.8.

IEEE ENGINEERING IN
MEDICINE AND BIOLOGY
Magazine

VOLUME 24 • NUMBER 5 ■ http://EMB-Magazine.bme.uconn.edu ■ SEPTEMBER/OCTOBER 2005